To: Vought-Sikorsky Aircraft,
Division of United Aircraft Corp.
Att: Mr Charles J McCarthy,
General Manager

61

234

ACR- Sept. 1942
#: 234

NATIONAL ADVISORY COMMITTEE FOR AERONAUTICS

ADVANCE CONFIDENTIAL REPORT #234

TESTS OF AN NACA 66,2-420 ~ 66(218)-420
AIRFOIL OF 5-FOOT CHORD AT HIGH SPEED

By Manley J. Hood and Joseph L. Anderson

Ames Aeronautical Laboratory
Moffett Field, Calif.

SR-234

September 1942

NATIONAL ADVISORY COMMITTEE FOR AERONAUTICS

ADVANCE CONFIDENTIAL REPORT

TESTS OF AN NACA 66,2-420 AIRFOIL OF 5-FOOT CHORD AT HIGH SPEED

By Manley J. Hood and Joseph L. Anderson

SUMMARY

This report covers tests of a 5-foot model of the NACA 66,2-420 low-drag airfoil at high speeds including the critical compressibility speed. Section coefficients of lift, drag, and pitching moment, and extensive pressure-distribution data are presented.

The section drag coefficient at the design lift coefficient of 0.4 increased from 0.0042 at low speeds to 0.0052 at a Mach number of 0.56 (390 mph at 25,000 ft altitude). The critical Mach number was about 0.60. The results cover a Reynolds number range from 4 millions to 17 millions.

INTRODUCTION

Tests have been made of an NACA 66,2-420 airfoil in order to provide data on the characteristics of a thick low-drag airfoil at high speeds. The NACA 66,2-420 airfoil was chosen as being representative of low-drag airfoils of rather high camber (0.40 design lift coefficient) and thickness (20 percent of the chord). The airfoil was tested at speeds up to and slightly above the critical speed.

APPARATUS AND METHOD

The tests were conducted in the NACA 16-foot wind tunnel at the Ames Aeronautical Laboratory, Moffett Field, California. This wind tunnel has a closed circular test section 16 feet in diameter.

The airfoil was of the NACA 66,2-420, a = 1 section. In the usual manner this airfoil designation signifies that the airfoil is a low-drag airfoil of the 6 family, that falling pressures extend from the leading edge to a point 60 percent of the chord from the leading edge over a working c_l range of approximately ±0.2 from the design lift coefficient, that the design lift coefficient is 0.4, that the airfoil thickness is 20 percent of the chord, and that the lift at the design lift coefficient is uniformly distributed across the chord. The coordinates of the airfoil section are shown in figure 1. These coordinates were derived from the coordinates of the NACA 66,2-018 airfoil as given in reference 1, by the method explained there. The airfoil had a constant chord of 5 feet and completely spanned the test section as shown in figure 2. Between the ends of the airfoil and the tunnel walls the clearance was approximately 3/16 inch. The airfoil spar extended through openings in the tunnel walls to trunnions which supported the airfoil and permitted changing the angle of attack. Except for the steel spar, the airfoil was of wood. The surface was painted, sandpapered smooth, and polished. A smooth, accurate surface was maintained throughout the tests. The angle of attack was checked during the tests by means of a torque tube extending through the airfoil to the center of the span where it was anchored. By this means the true angle at the center of the span was always determined and errors due to elastic twisting of the airfoil were eliminated.

All drag coefficients were computed from measurements of the momentum loss in the wake of the airfoil. The measurements were made 3 feet behind the trailing edge at the center of the span by means of a rake of total-pressure and static-pressure tubes connected to a multiple manometer. The pressures were recorded by photographing the manometer. The drag coefficients were computed by Jones' method modified to include compressibility effects.

The static-pressure distribution was measured with flush orifices built into the airfoil 2.5 feet to the right of the center of the span. The pressures were recorded by photographing a multiple manometer to which the orifices were connected.

The lift coefficients were derived by integrating plots of the pressure distribution to obtain the coefficient of normal force, and then resolving the normal force coefficient and the drag coefficient in accordance with the angle of attack to obtain the lift coefficient. Coefficients of pitching moment were computed from integrated moments of chordwise and spanwise pressure-distribution plots.

For a few of the tests the transition point was arbitrarily fixed at 10 or 60 percent chordwise positions on both upper and lower surfaces by spanwise bands of carborundum grains. The bands of carborundum were approximately 1/2 inch wide and the grain size was number 60.

RESULTS AND DISCUSSION

All results are shown as section properties of the airfoil in terms of the usual non-dimensional coefficients. No corrections have been made for the constricting effect of the wind-tunnel walls. It is estimated that the errors due to the omission of these corrections do not exceed 2 percent at low speeds and 4 percent at the highest speeds. These errors tend to indicate the coefficients as too large numerically, thus giving conservative values for most uses.

The characteristics of the airfoil at 0 degree angle of attack are shown in figures 3 and 4 as they vary with Mach number and Reynolds number, respectively. The section drag coefficient for the smooth airfoil was only 0.0042 at low speeds and increased gradually to 0.0052 as the Mach number and Reynolds number were increased to 0.56 and 16,500,000, respectively. The minimum pressure coefficients plotted in figure 5 indicate that the critical Mach number was 0.6, and this value is confirmed by the break in the curve showing lift coefficient on figure 3. The drag started increasing rapidly at Mach numbers above 0.56, however, and at a Mach number of 0.60 the drag coefficient was double its low-speed value. At a Mach number of 0.633 the drag coefficient had increased to six times its low-speed value. The major portion of this large drag increase is believed to be the result of compressibility shock. At the high Mach numbers the adverse pressure gradients over the after 40 percent of the chord become very large and may have caused separation which would contribute to the increase in drag.

As compared to the smooth wing, roughness at the 60-percent chord station caused an almost constant increase in the drag coefficient, about 0.0009, at all Mach numbers up to 0.56. This comparison indicates that the natural transition point was aft of the 60-percent station (the minimum pressure point) at least until the critical Mach number was approached. The results do not show how far the Reynolds number can be increased before the transition point moves forward and the drag increases due to scale effect. Tests of a larger chord airfoil of the same section are to be made in order to evaluate the capabilities of this airfoil at higher Reynolds numbers.

With the smooth airfoil at 0 degree angle of attack the pitching-moment coefficient remained within 0.02 of the theoretical value of -0.10 throughout the range of the tests. Only a small change in $c_{m_{c/4}}$ occurred at the critical speed. The lift coefficient, theoretically 0.40, increased from approximately 0.38 at low speeds to 0.48 at the critical speed and then decreased rapidly above the critical speed. Compared to the experimental increase from 0.38 to 0.48, the theory of Prandtl and Glauert that the lift increases with Mach number as $1/\sqrt{1-M^2}$ would predict an increase to 0.465.

Fixing the transition point at 60-percent chord had unimportant effects on the lift and pitching moment. Fixing the transition point at 10-percent chord increased the minimum drag coefficient to 0.0106, decreased the lift coefficient by 0.1 or more, and increased the pitching moment coefficient by 0.025 or more. These changes are indicative of what might occur if the transition takes place prematurely due to faulty wing construction, deterioration of the wing contour or smoothness in service, interference, or other causes.

The characteristics of the smooth airfoil at various angles of attack are shown in figure 6 in terms of Mach number and in figure 7 in terms of Reynolds number. Figure 8 presents cross-plots taken from figure 6 and shows, for a Mach number of 0.4, the variation of lift with angle of attack and the variation of drag and pitching moment with lift. These figures show that the drag remains low for lift coefficients from approximately 0.35 to 0.55 and increases to higher values for lift coefficients outside of this range. For the conditions of these tests the airfoil did not retain its low-drag characteristics over quite as wide a range of lift coefficients as is indicated by the airfoil designation (±0.2). In practice the range of lift coefficients over which the low-drag persists can be extended by the use of flaps with small deflection. From figures 6 and 9 it is evident that the critical Mach number increases slightly as the angle of attack is decreased to -2°, and decreases as the angle of attack is increased above $+2^{\circ}$. The reason for the change in critical speed with angle of attack is evident from the plots of pressure distribution.

The variation of the minimum pressure coefficient S with Mach number for different airfoil conditions is shown in figures 5 and 9. There are also shown curves of critical pressure coefficients S_{cr} the values at which the speed of sound is reached locally. The intersections of the pressure-coefficient curves with the critical curve indicate the critical Mach numbers at which sonic velocity is reached locally. In figure 5 there are also shown two curves of von Kármán's theoretical equation for the rate of increase of pressure coefficient with Mach number (reference 2). With the smooth airfoil the pressures increased more rapidly with Mach number than would have been predicted from the theory; consequently, predictions based upon the results of low-speed tests would overestimate the critical speed. With the transition fixed by roughness at 10-percent chord, the pressures were less throughout the speed range and increased less rapidly as the speed was increased. These differences probably resulted from changes in the effective shape of the airfoil caused by the thicker boundary layer with the forward transition.

Figure 10 shows the section normal force and pitching moment coefficients for angles of attack from below the negative stall to above the positive stall for the smooth airfoil and also with roughness fixing the transition at the 10-percent chord position. The maximum positive and negative normal force coefficients were +1.50 and -1.35, respectively, and were unaffected by the roughness.

Figures 11 to 17, inclusive, present pressure-distribution data for various Mach numbers, angles of attack, and transition locations. These data are useful for computing structural loads, and for estimating induced velocities, pressure gradients, and critical speeds when the airfoil is combined with other bodies.

CONCLUSIONS

The section drag coefficient of the airfoil at the design lift coefficient of 0.4 increased from 0.0042 at low speeds to 0.0052 at a Mach number of 0.56, above which the drag increased rapidly.

Ames Aeronautical Laboratory,
National Advisory Committee for Aeronautics,
Moffett Field, Calif.

REFERENCES

1. Jacobs, Eastman N., Abbott, Ira H., and Davidson, Milton: Preliminary Low-Drag-Airfoil and Flap Data from Tests at Large Reynolds Numbers and Low Turbulence. A.C.R., NACA, March 1942.

2. von Kármán, Th.: Compressibility Effects in Aerodynamics. Journal of the Aeronautical Sciences, vol. 8, no. 9, July 1941, pp. 337-56.

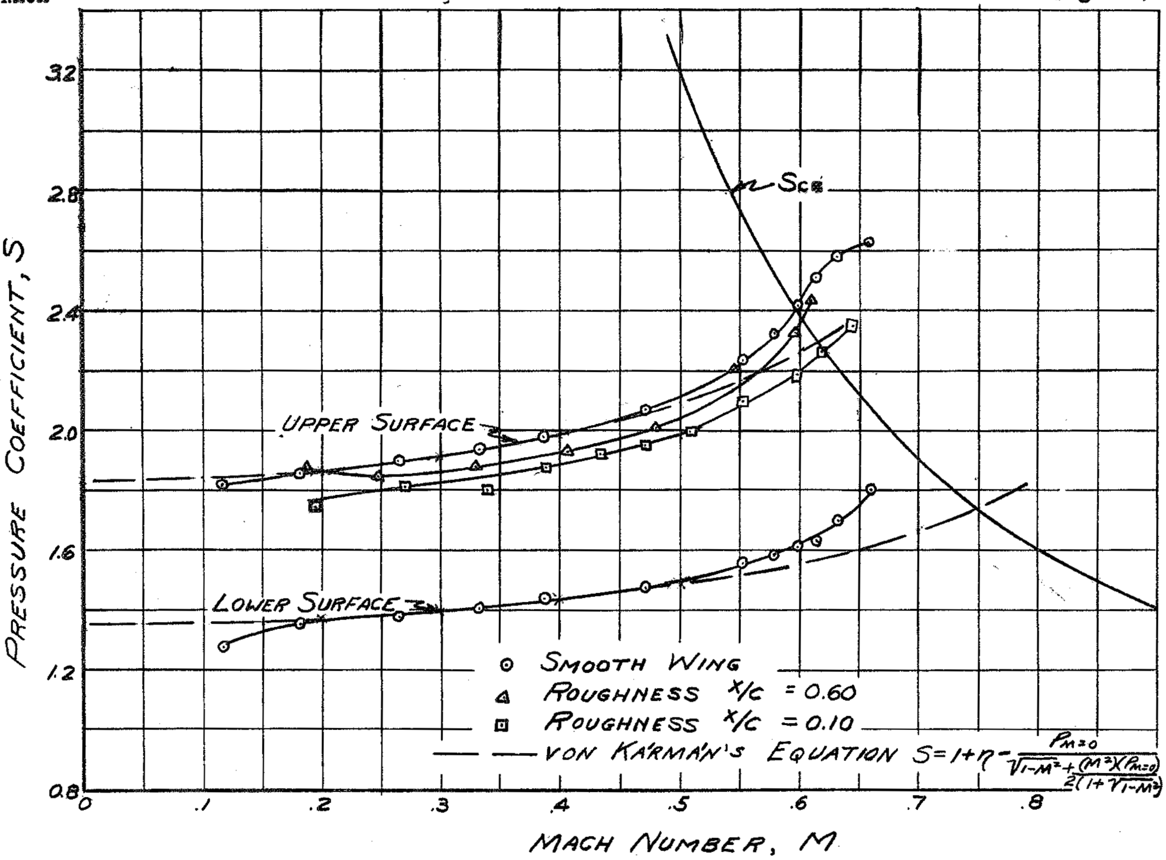

Figure 5.- Effect of compressibility and surface condition on the minimum pressure coefficients. $\alpha = 0^{\circ}$

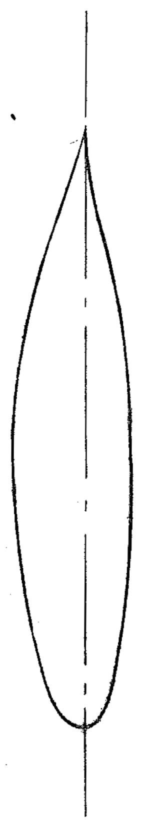

5' chord

α = 1 see page 2 (top)

Upper Surface Station	Upper Surface Ordinate	Lower Surface Station	Lower Surface Ordinate
0	0	0	0
0.235	1.676	0.765	-1.476
0.455	2.039	1.045	-1.759
0.916	2.613	1.584	-2.185
2.122	3.614	2.878	-2.870
4.587	5.039	5.413	-3.775
7.074	6.169	7.926	-4.473
9.575	7.115	10.425	-5.047
14.599	8.603	15.401	-5.911
19.640	9.742	20.360	-6.558
24.691	10.626	25.390	-7.046
29.748	11.295	30.252	-7.407
34.809	11.770	35.191	-7.650
39.872	12.067	40.128	-7.783
44.936	12.188	45.064	-7.808
50.000	12.135	50.000	-7.723
55.062	11.871	54.938	-7.491
60.119	11.381	59.881	-7.097
65.167	10.535	64.833	-6.415
70.200	9.338	69.800	-5.450
75.215	7.923	74.785	-4.340
80.211	6.367	79.789	-3.183
85.186	4.704	84.814	-2.012
90.139	3.017	89.861	-0.949
95.069	1.375	94.931	-0.111
100.000	0	100.000	0

L.E. RAD. 2.83

Figure 1.- Coordinates of the NACA 66,2-420 airfoil in percent of chord.

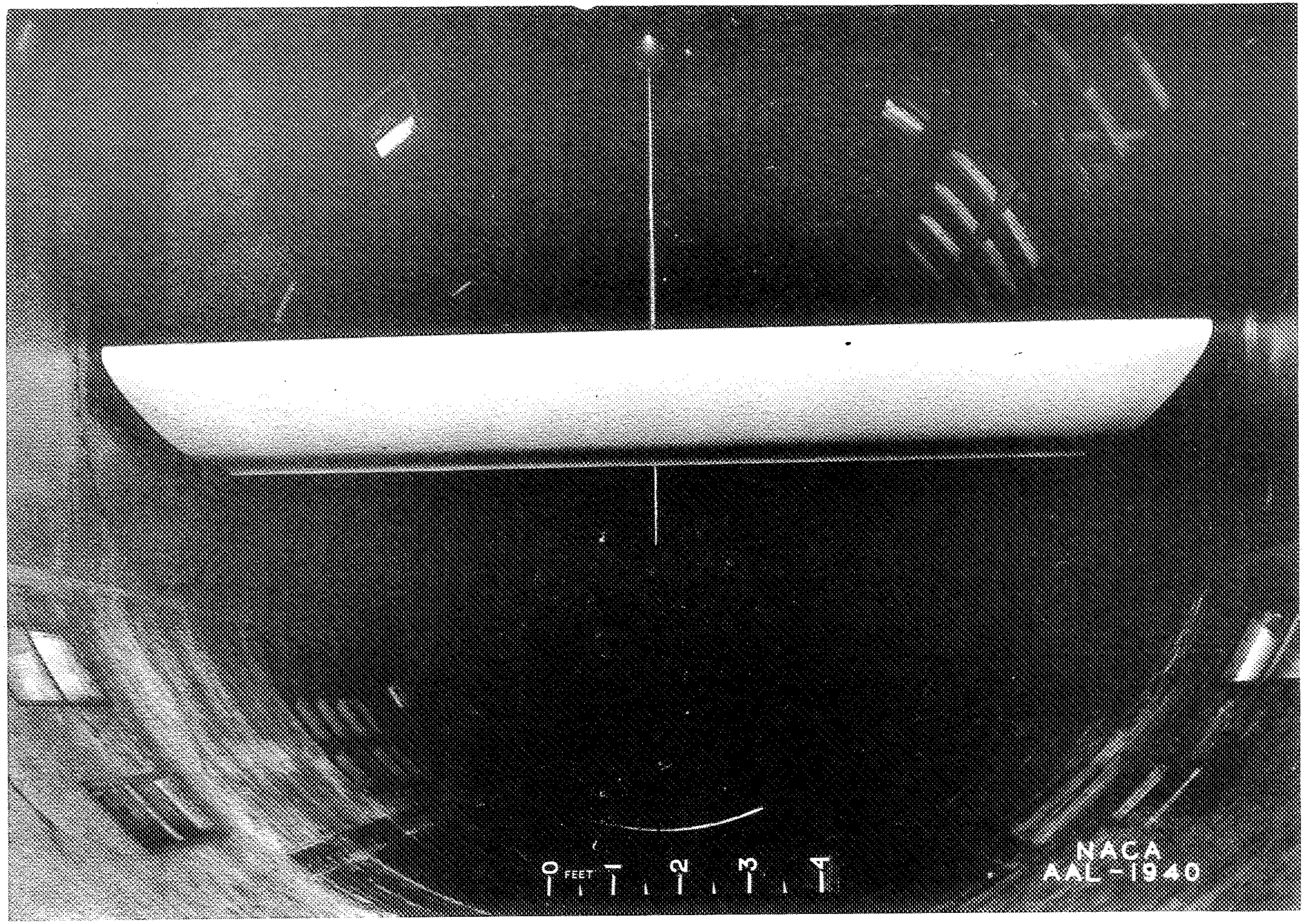

Figure 2.- NACA 66,2-420 airfoil in the wind tunnel with the momentum rake in place.

5' chord
16' span

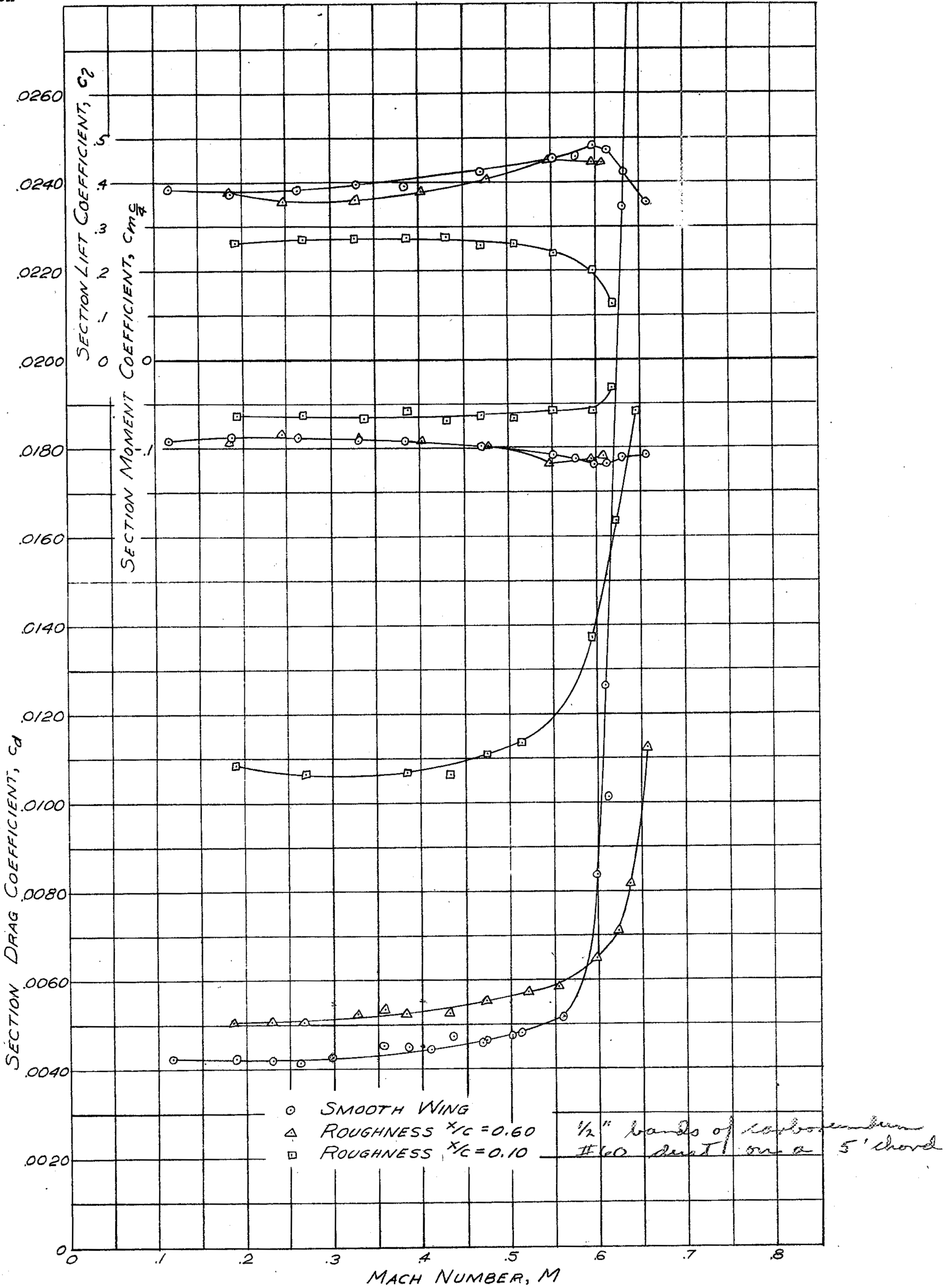

Figure 3.- Variation of the section coefficients with Mach number for various surface conditions. $\alpha = 0^{\circ}$

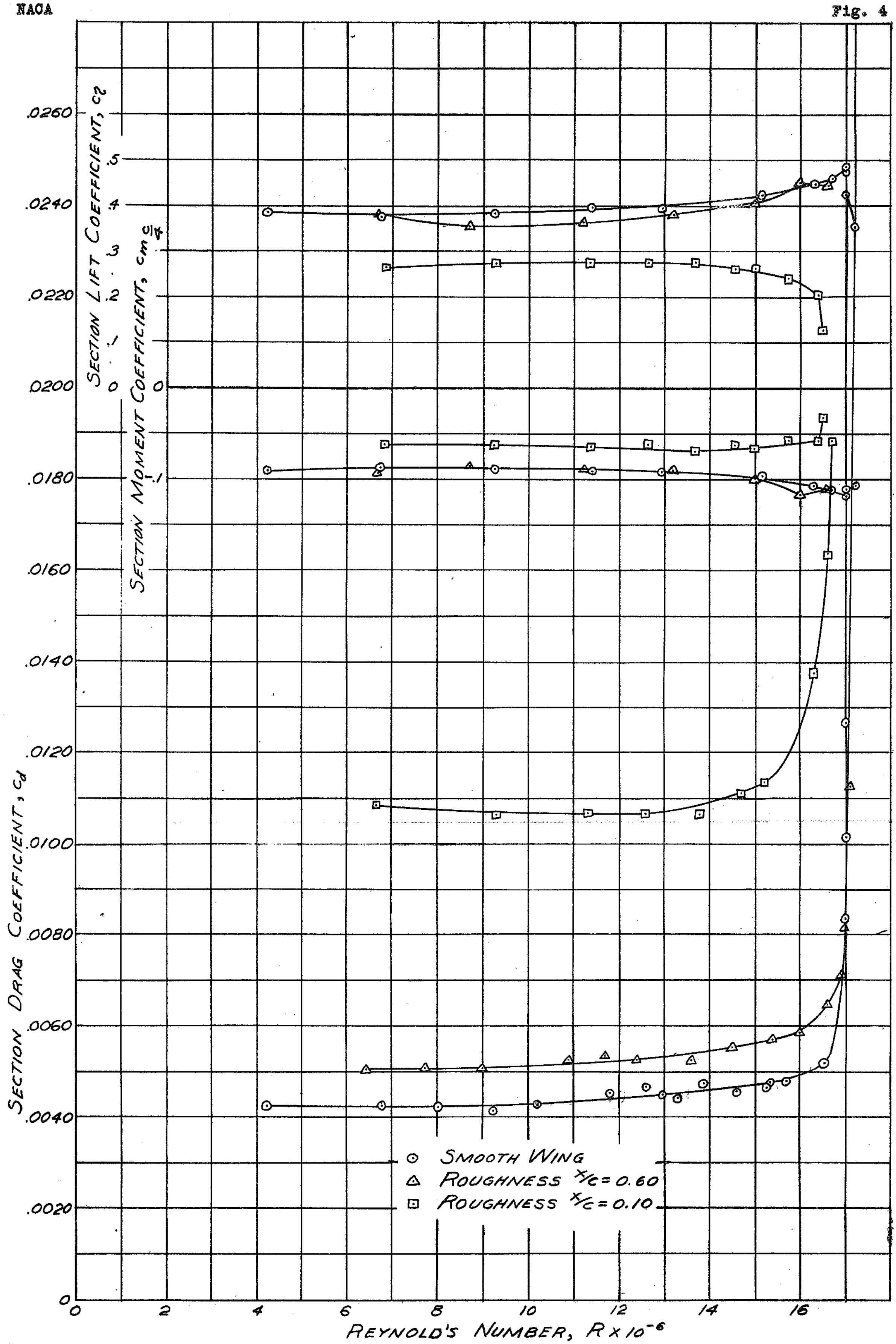

Figure 4.- Variation of the section coefficients with Reynolds number for various surface conditions. $\alpha = 0^{\circ}$

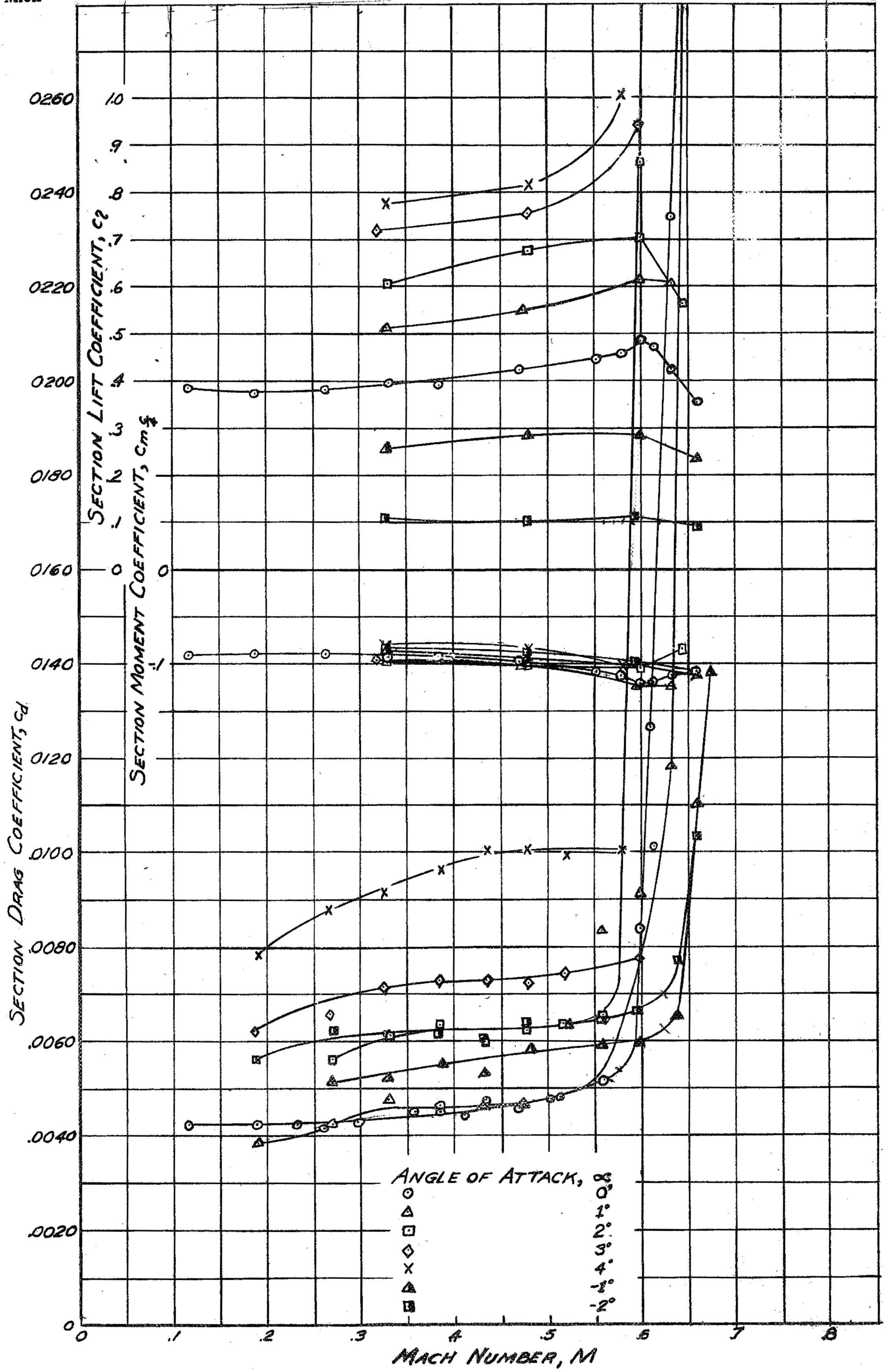

Figure 6.- Variation of section coefficients with Mach number and angle of attack.

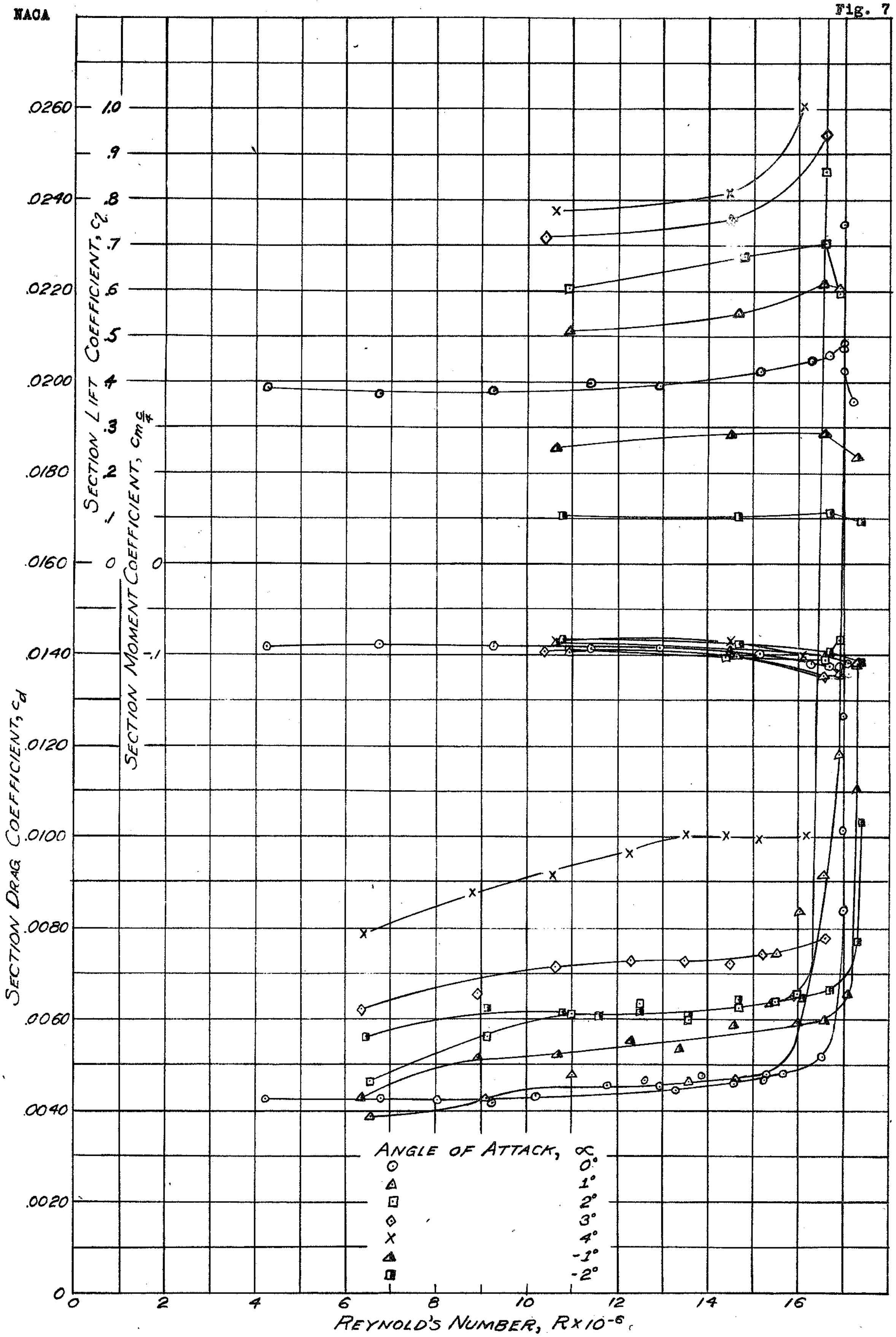

Figure 7.- Variation of section coefficients with Reynolds number and angle of attack.

NACA

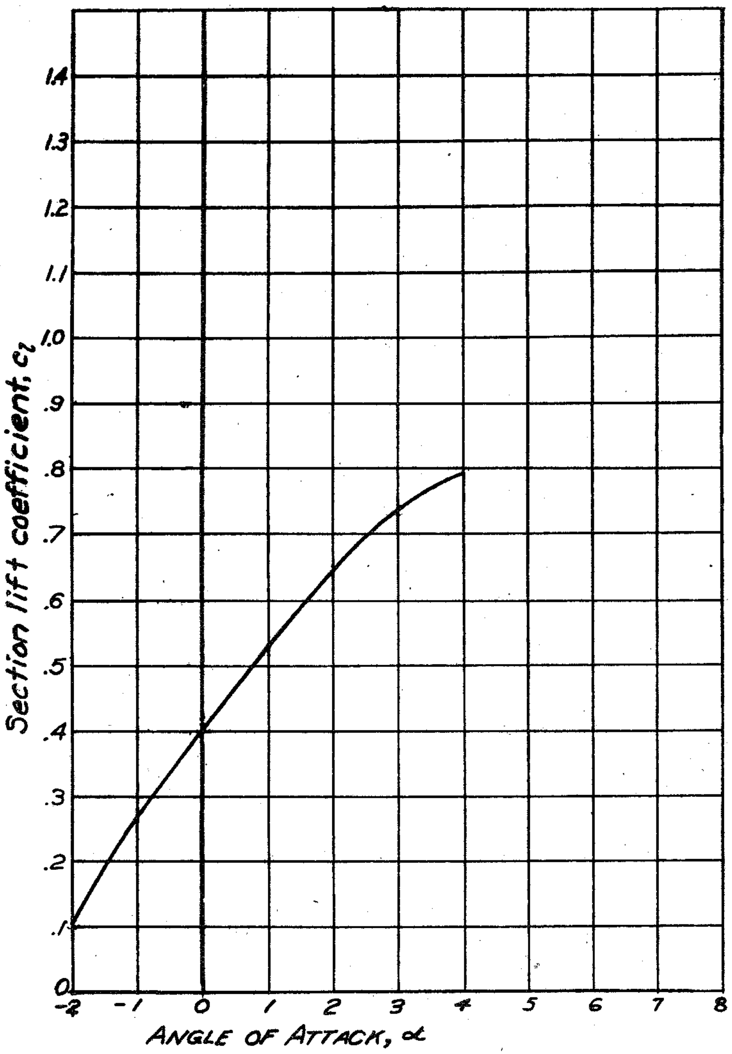

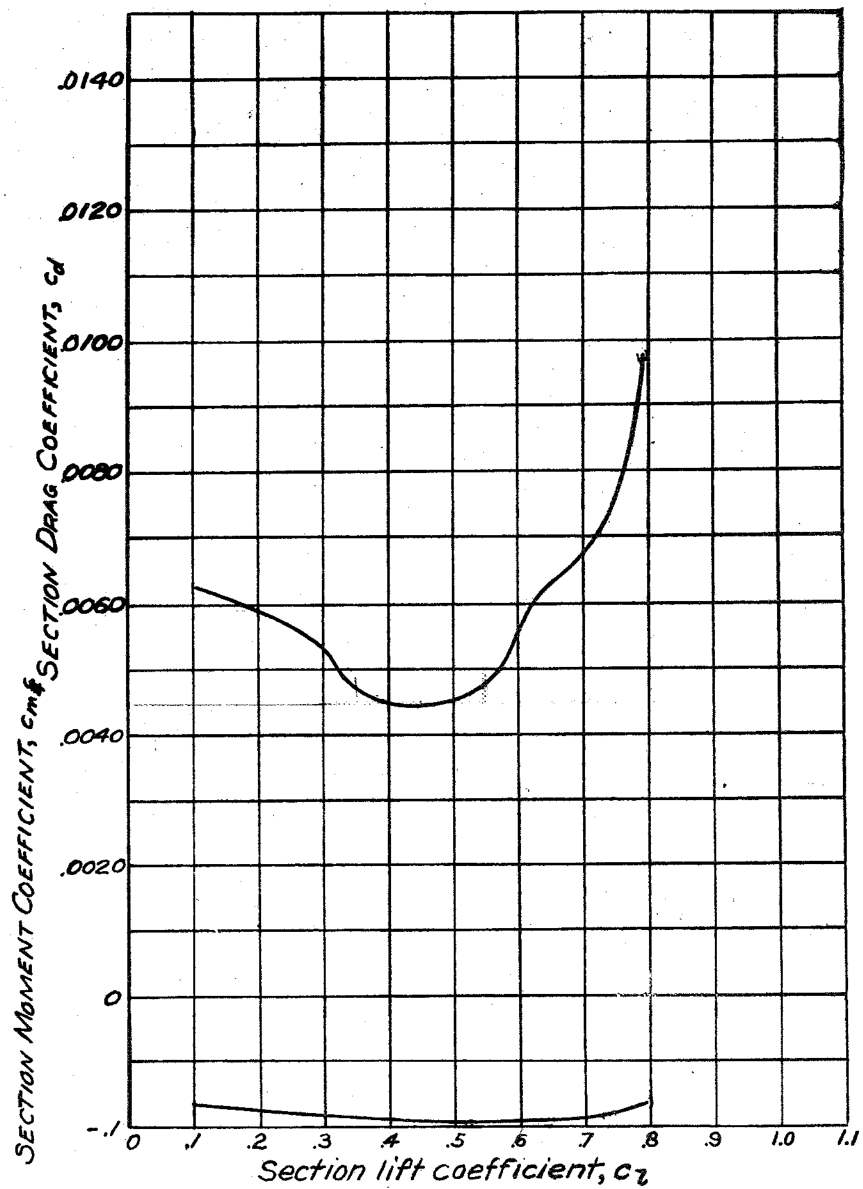

Figure 8.- Polar of section coefficients for smooth airfoil. Mach number = 0.40.

Fig. 8

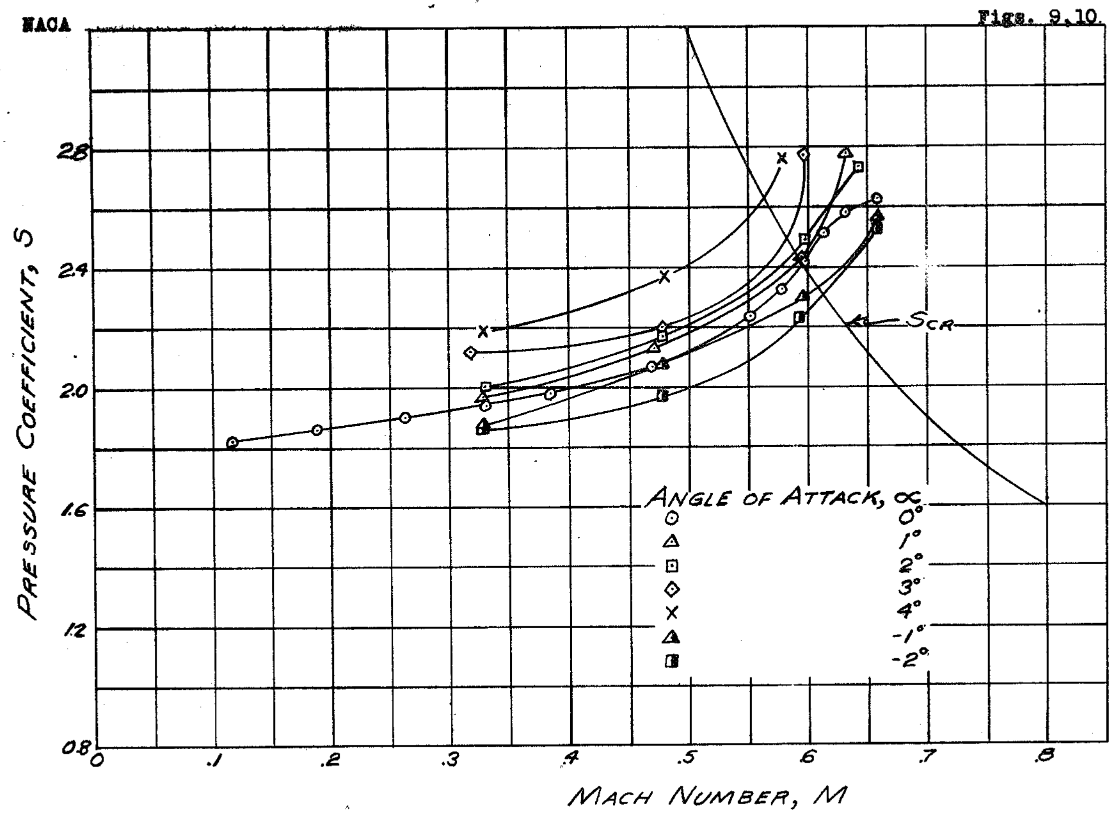

Figure 9.- Effect of compressibility and angle of attack on the minimum pressure coefficient of the upper surface.

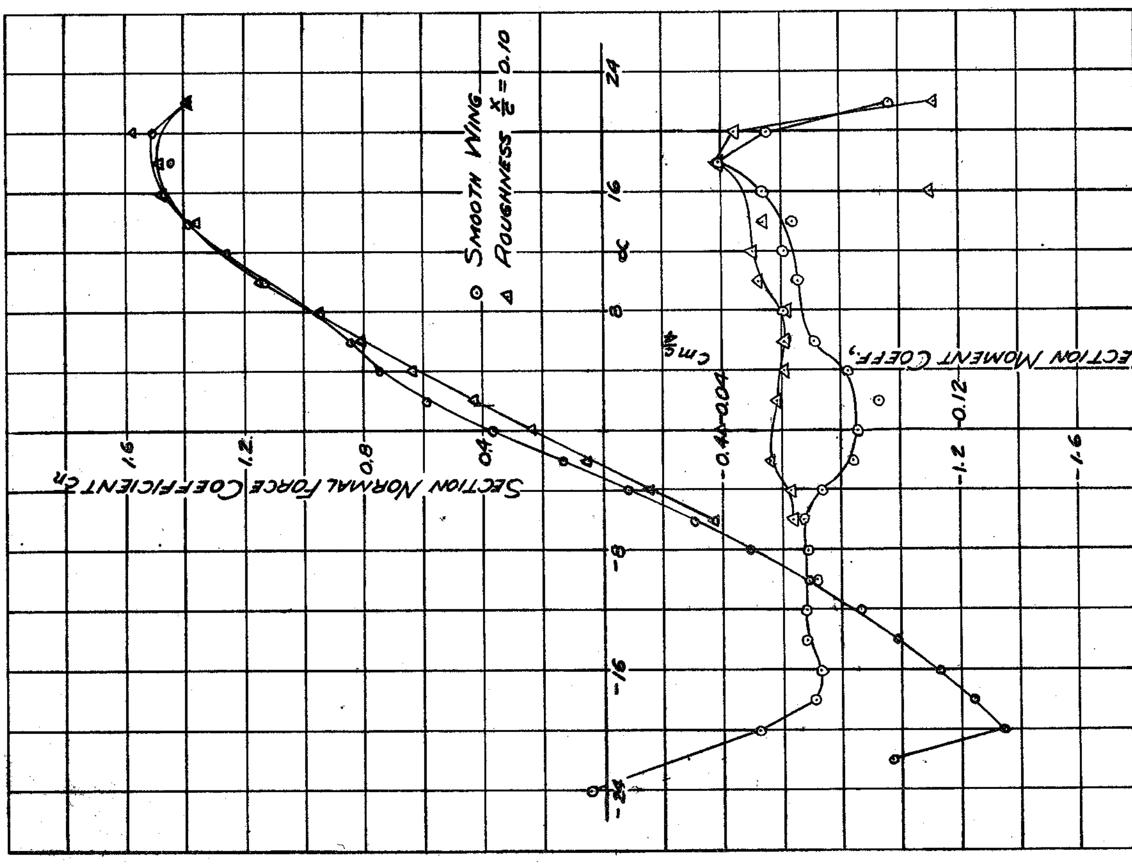

Figure 10.- Variation of section coefficients with angle of attack. Mach number = 0.185.

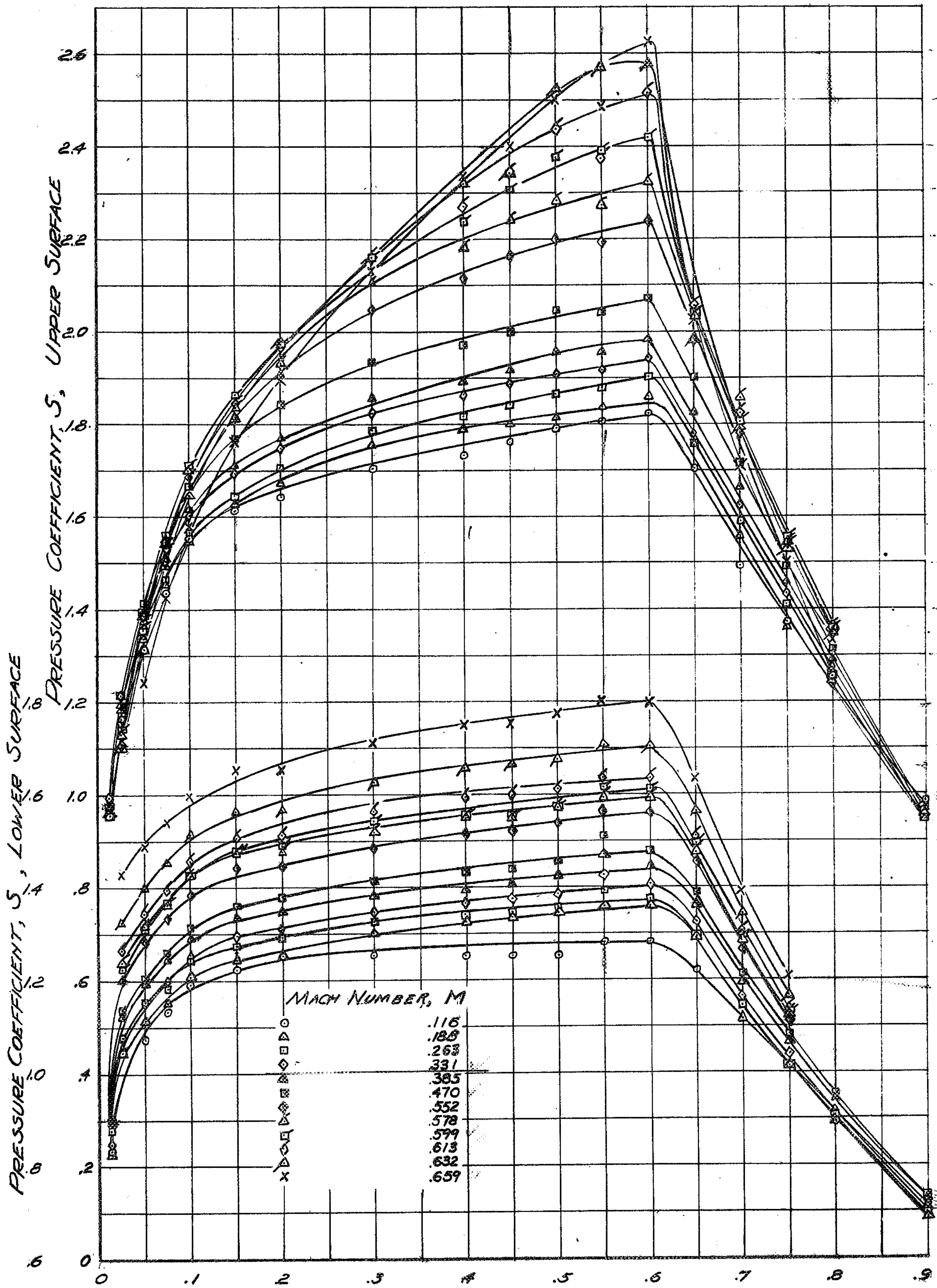

Figure 11.- Pressure distribution on the smooth airfoil. $\alpha = 0^{\circ}$.

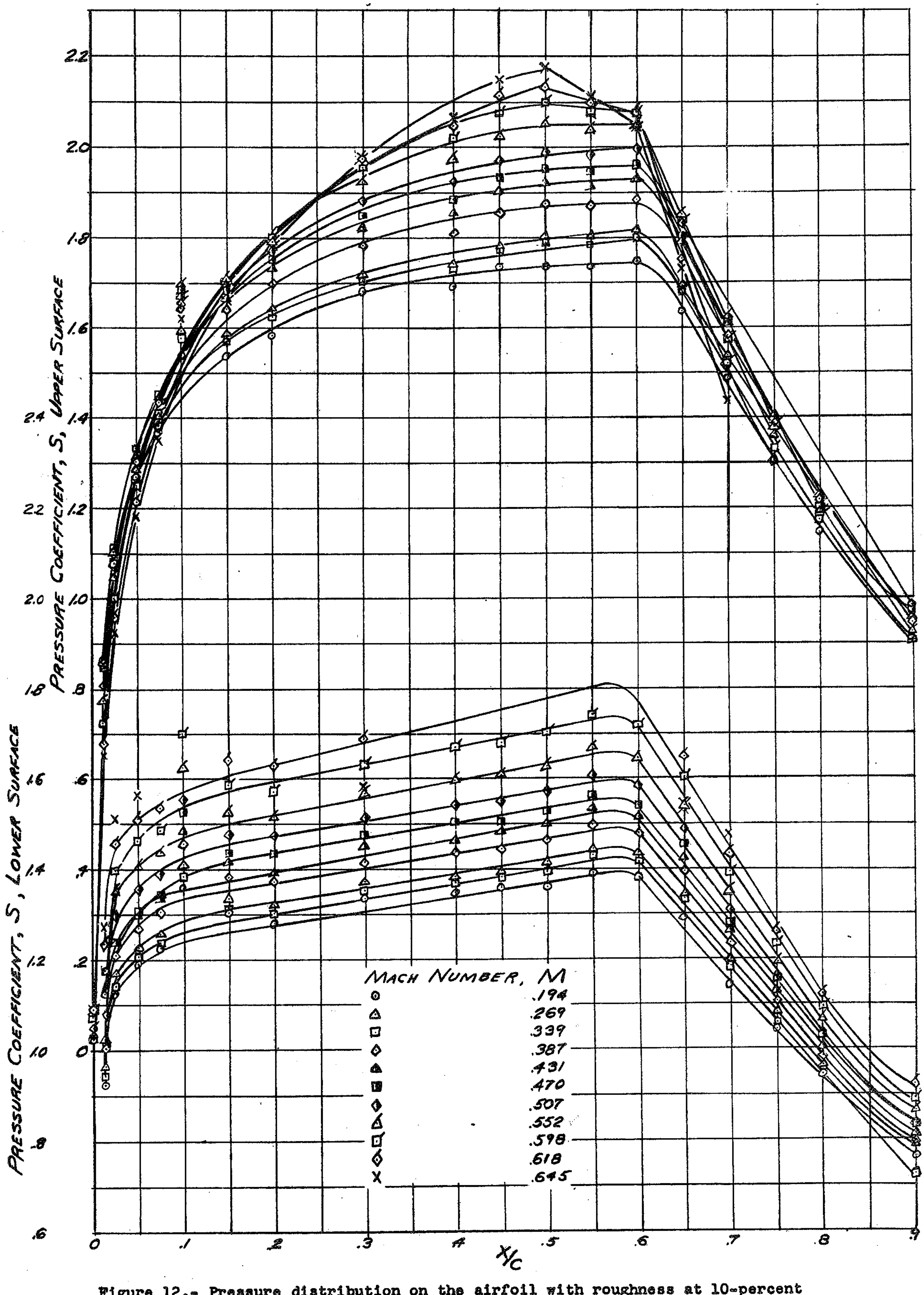

Figure 12.- Pressure distribution on the airfoil with roughness at 10-percent chord. $\alpha = 0°$.

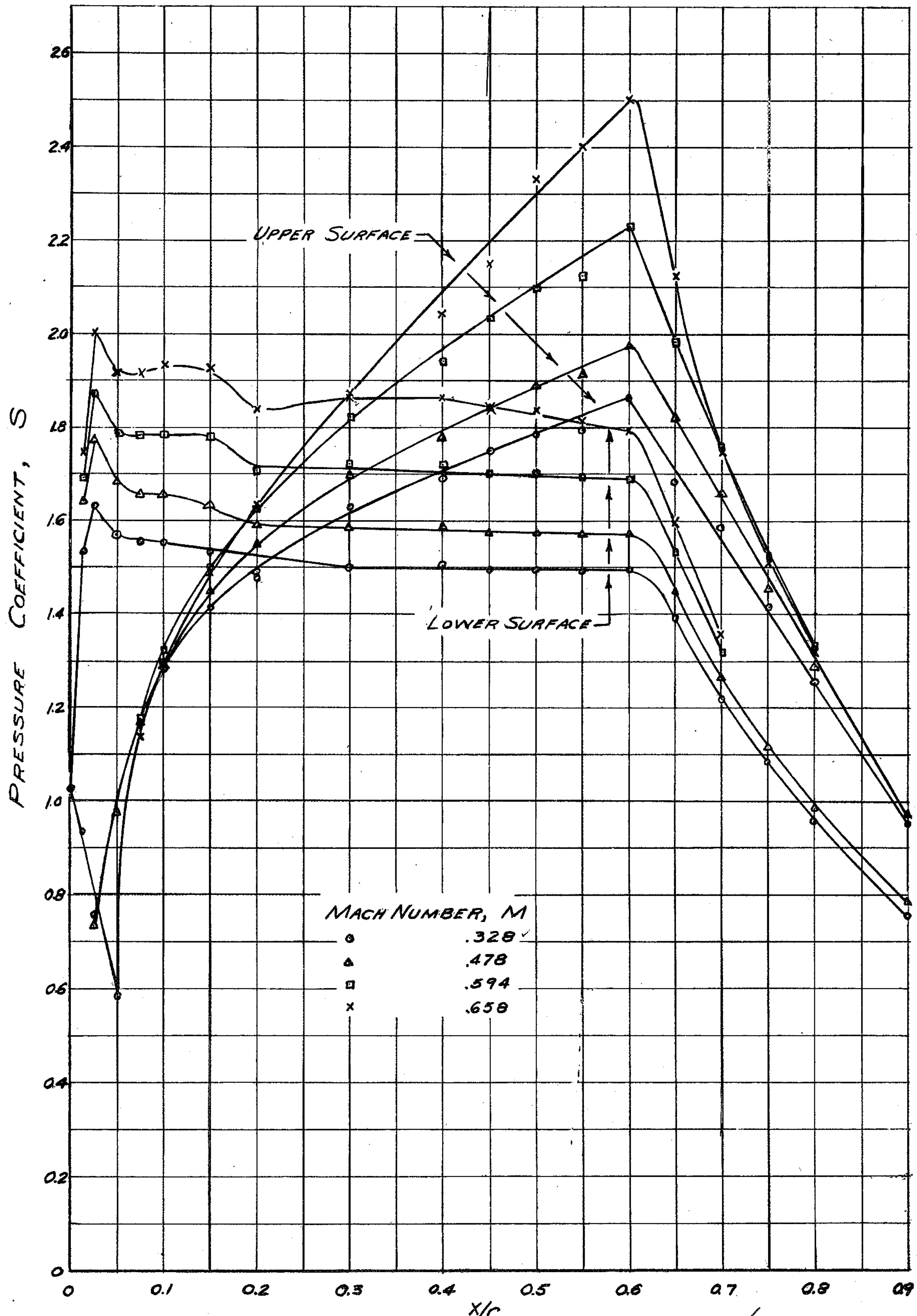

Figure 13.- Pressure distribution on the smooth airfoil. $\alpha = -2^{\circ}$.

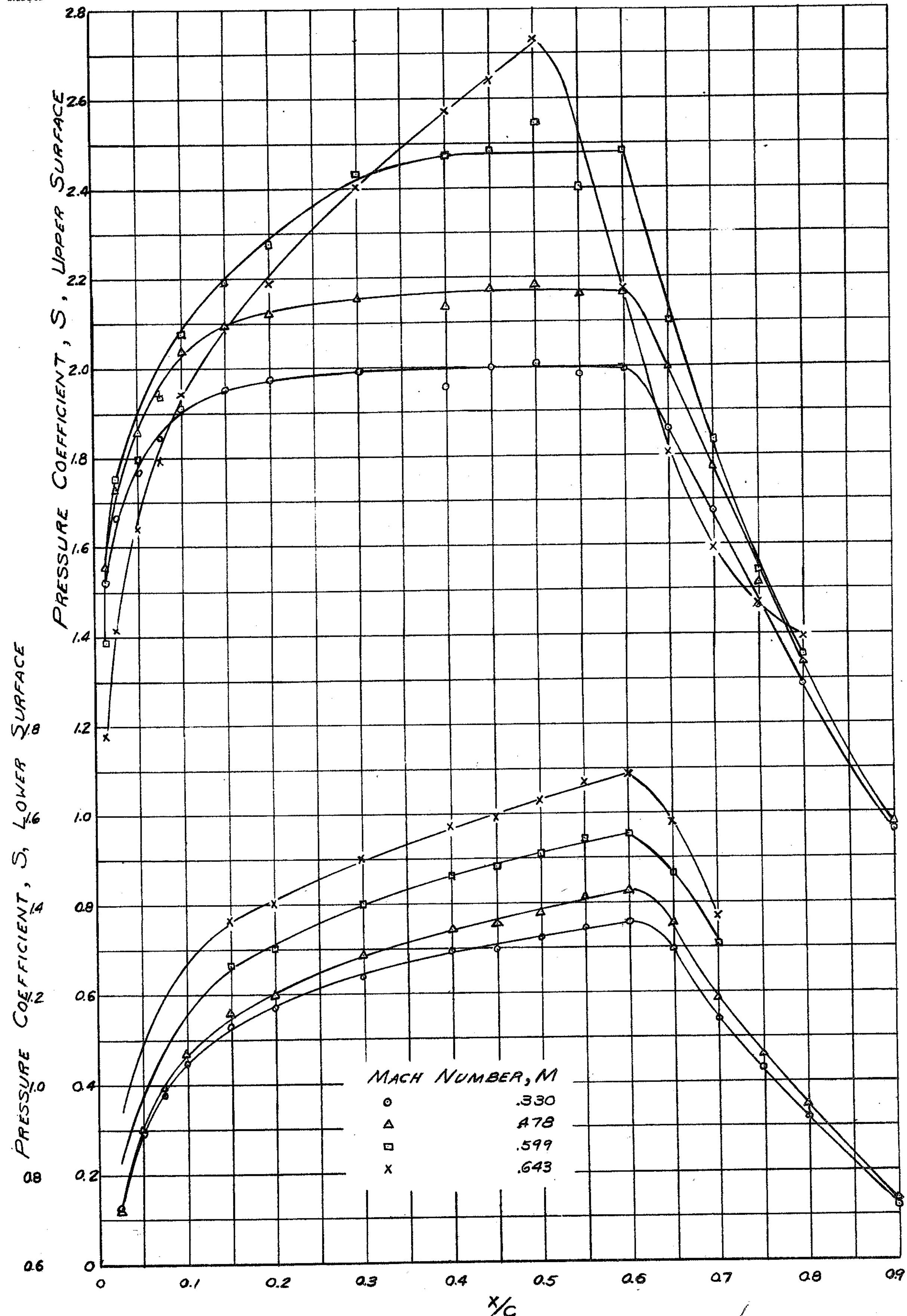

Figure 14.- Pressure distribution on the smooth airfoil. $\alpha = +2^\circ$

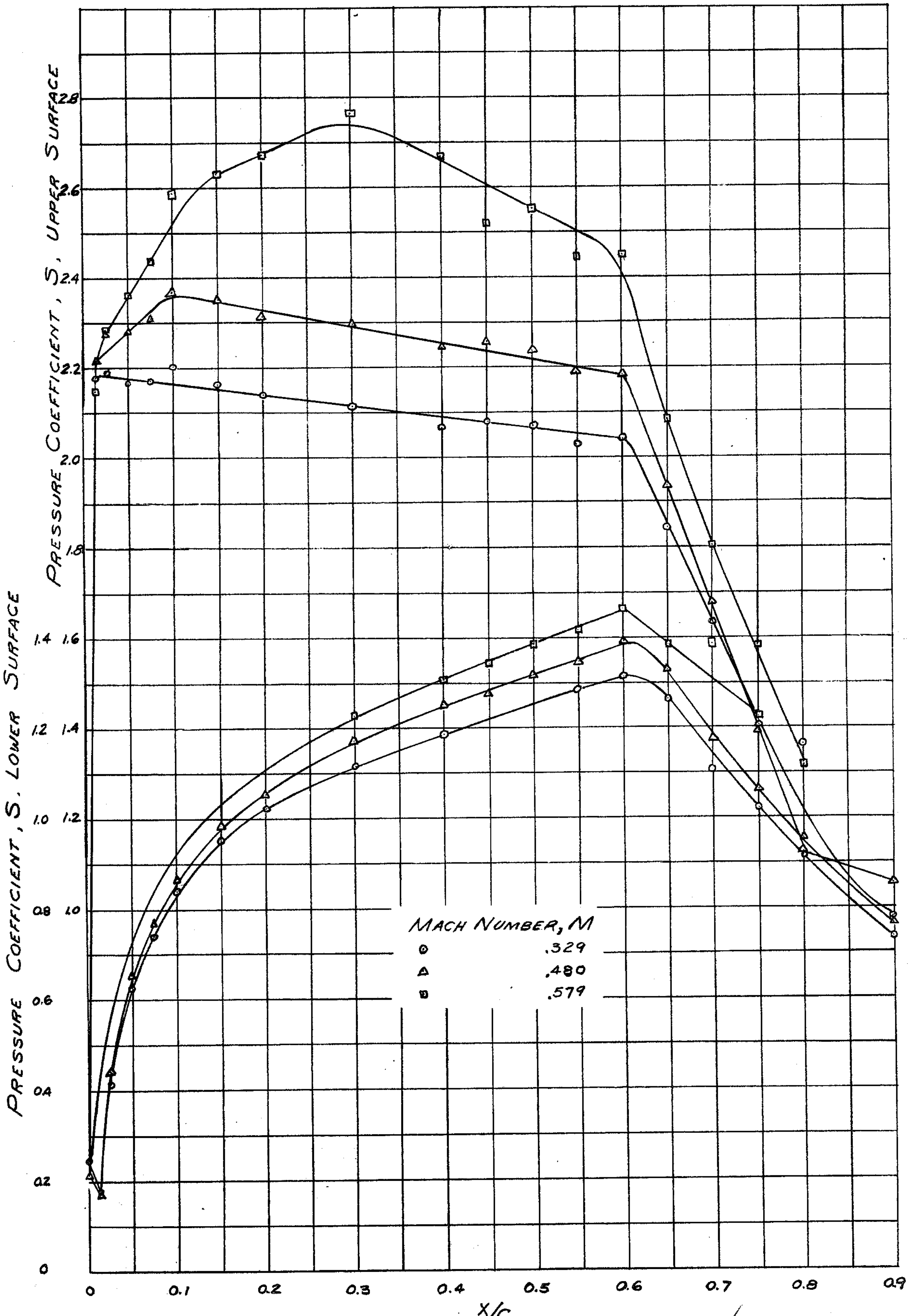

Figure 15.- Pressure distribution on the smooth airfoil. $\alpha = +4^{\circ}$.

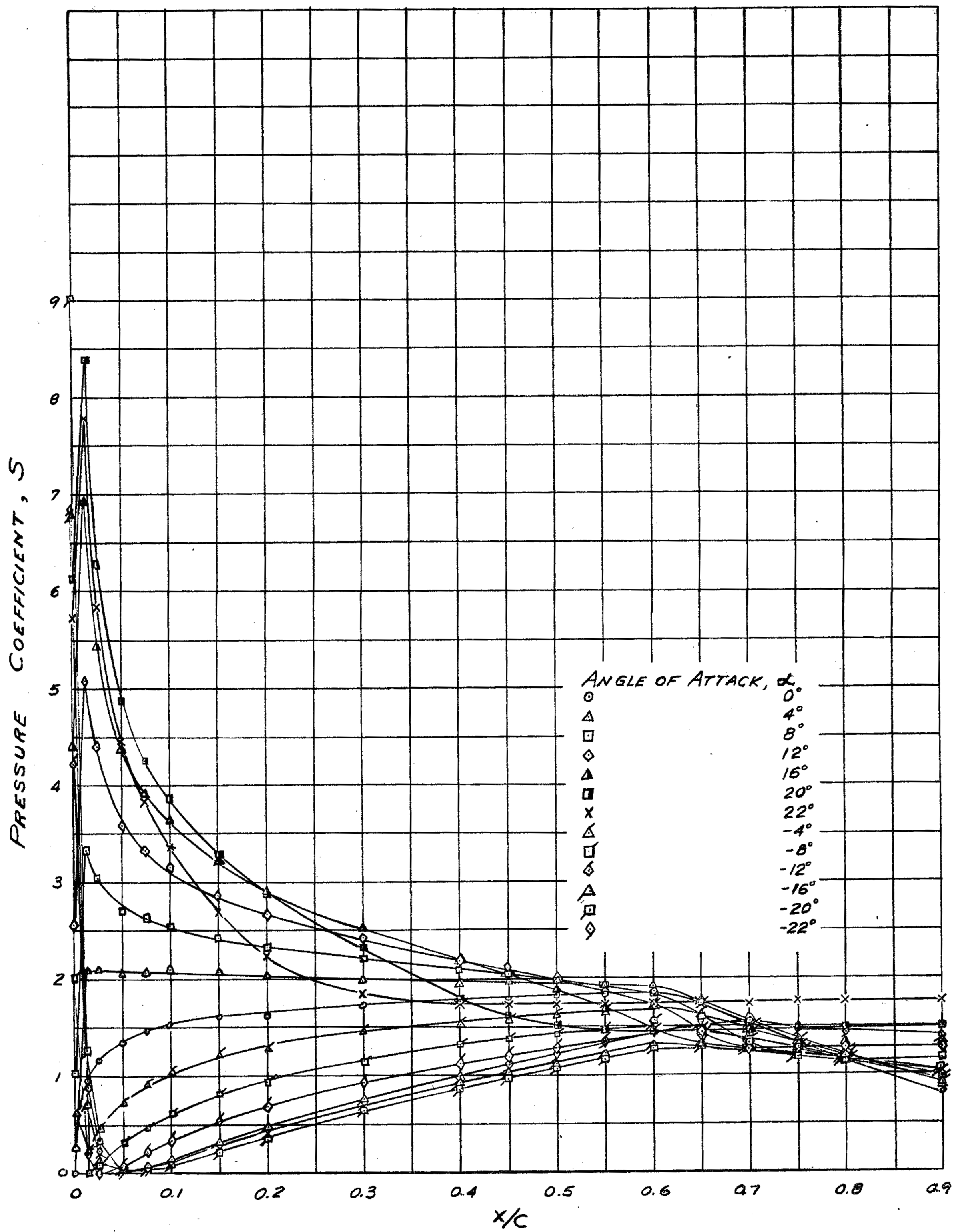

Figure 16.- Variation of the pressure coefficient for the upper surface with angle of attack. Mach number = 0.185.

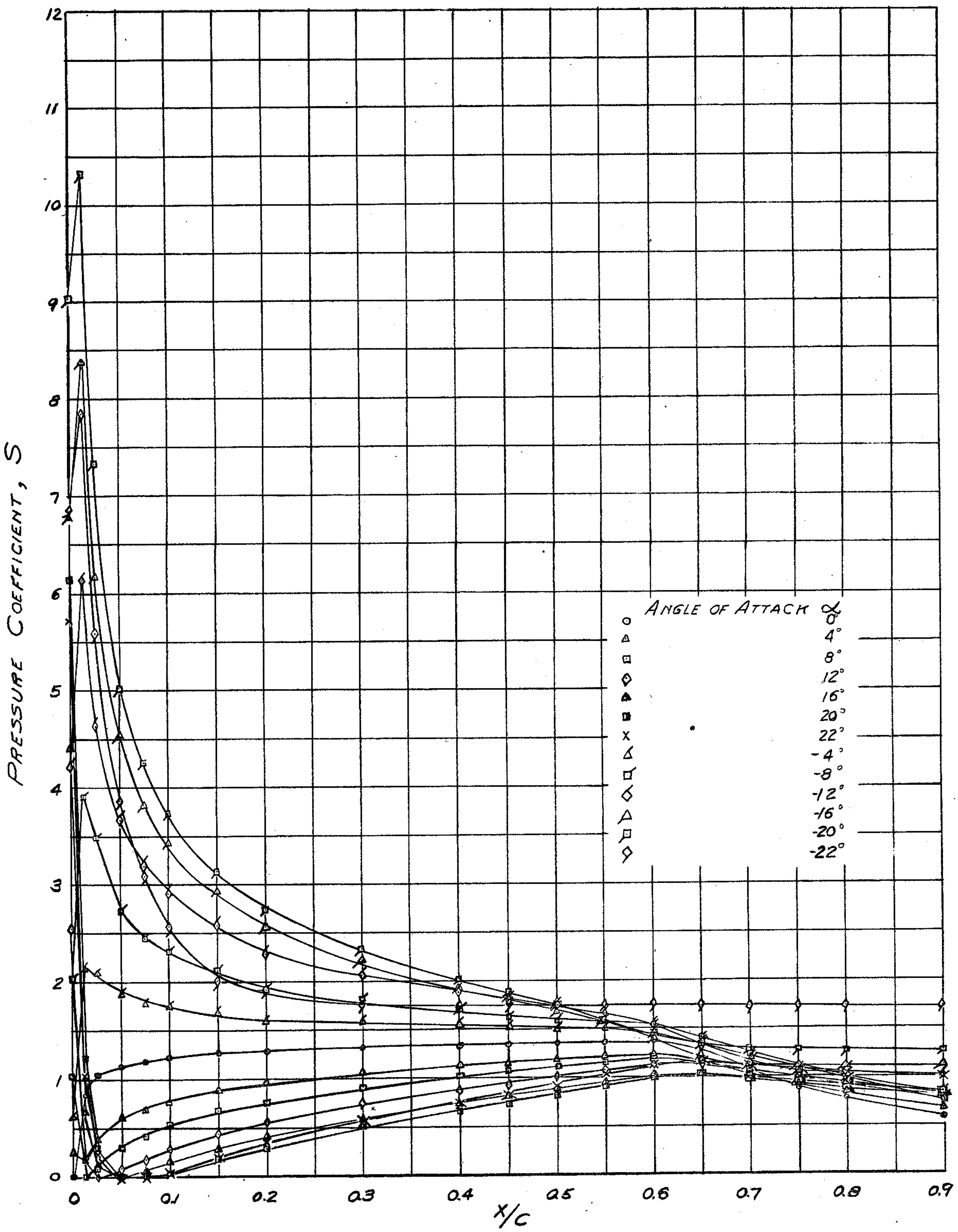

Figure 17.- Variation of the pressure coefficient for the lower surface with angle of attack. Mach number = 0.185.